H2Open Journal

IWA PUBLISHING

H2Open Journal Vol 5 No 4, 713 doi: 10.2166/h2oj.2022.045

Bioleached laterite nano iron catalyst (BLaNFeCs)-based Fenton's degradation of selective dyes in water

Bhaskar Shivaswamy [a,*], Basavaraj Manu [a] and M. Y. Sreenivasa [b]

[a] Department of Civil Engineering, National Institute of Technology Karnataka, Surathkal, P.O. Srinivasnagar, Mangalore 575025, India
[b] Department of Studies in Microbiology, University of Mysore, Mysuru 570006, Karnataka, India
*Corresponding author. E-mail: baskarmalwanitk@gmail.com

BS, 0000-0002-0203-3629

ABSTRACT

Iron nanocatalyst for its potential application as Fenton's catalyst for the degradation of methylene blue dye was synthesized with the fruit extract of *Citrus maxima* using bioleached laterite iron as a precursor. Synthesized iron particles were characterized suitably and their catalytic role in the degradation of methylene blue and rhodamine B by Fenton's oxidation was evaluated. The synthesized nanocatalyst exhibits heterogeneous catalytic properties in the degradation of methylene blue and rhodamine B with a degradation efficiency of 93.6 and 91.3%, respectively. Observed rate constants are consistent with the increase in catalyst dosage as it speeds up the reaction. The degradation of methylene blue and rhodamine B follows a pseudo-first-order reaction with a linear fit. Reusability studies confirm the reduction in the catalytic efficiency of the synthesized iron nanoparticles after five consecutive cycles.

Key words: *Citrus maxima*, dye, Fenton's process, laterite, methylene blue, rhodamine B

HIGHLIGHTS

- Synthesis and characterization of bioleached laterite nanoparticles.
- Fenton's oxidation.
- Degradation of selective dyes.
- Sustainable replacement of natural laterite iron for commercial iron.
- Reusability studies on the catalyst.

GRAPHICAL ABSTRACT

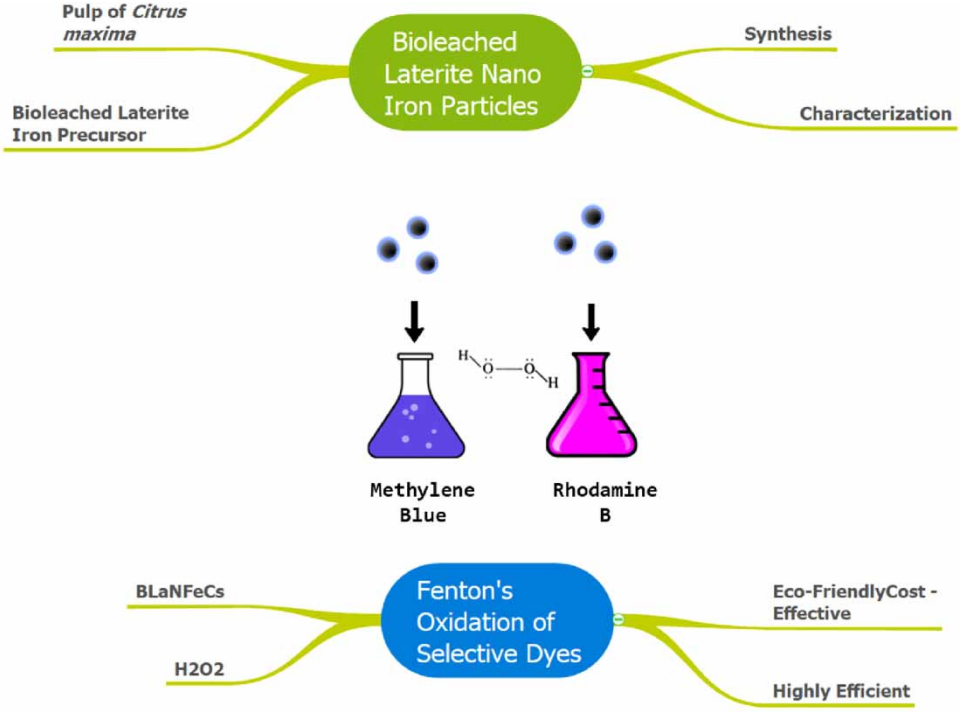

1. INTRODUCTION

Diverse chemical reagents used in the textile industries and large volume of water leads to the generation of wastewater contaminated with environmental persistent chemicals. Dyes by the virtue of their nature are non-amenable to degradation of exposure to water and other chemicals (Dutta & Mukhopadhyay 2001). Dyes usually have benzene and naphthalene rings but may also contain aromatic or aliphatic groups. It is the side group attached to the dye that imparts the color. It is the complex nature of dyes that makes them more interesting in the field of chemical remediation. Synthetic azo dyes are carcinogenic to humans in nature with potential toxic properties. Discharge of wastewater containing dye to natural streams and rivers may harm the biodiversity, posing toxicity to aquatic life (Islam & Mostafa 2018). Methylene blue belongs to the phenothiazine group of organic dyes. Discovered in the year 1876, methylene blue has its application as a tracer in the field of medicine for the radioactive detection of cancer (Nour n.d.; Simmons *et al.* 2003).

Many treatment methods like ozonation, electrochemical method, and the photochemical methods have been suggested for dye degradation out of which the photochemical method is proven to be effective because of its application and simplicity (Huang *et al.* 1993; Kim *et al.* 2004; Huang *et al.* 2008). Hydroxyl peroxide produced by the dissociation of hydrogen peroxides acts on the complex structure of organic dyes, breaking it, and causing degradation. The dissociation of hydrogen peroxide is a slow process for which a divalent cation, usually ferrous iron, is used to accelerate the reaction.

Various studies have been carried out on Fenton's oxidation of dyes in water and wastewater (Kim & Kan 2014). The generation of a large quantity of sludge and the cost of iron catalyst for the treatment are the limitations for the application of Fenton's oxidation on a large scale. Studies on the replacement of commercial iron from lateritic iron have been conducted and reported. However, the cost-effectiveness of chemical leaching remains in question. In this article, cost-effective bioleaching of lateritic iron for its application as Fenton's catalyst in the degradation of organic compounds is reported (Bhaskar *et al.* 2021).

Nanoparticles, being an effective tool in water and wastewater treatment, have an application in Fenton's oxidation. Heterogenous Fenton's oxidation using nano iron catalyst is much more effective in the degradation of organic compounds specific to organic dyes (Bishnoi *et al.* 2018). However, the efficiency of such treatment depends on the type of catalyst and method used in the synthesis of iron nanocatalyst.

The present study encompasses the synthesis and characterization of iron nanoparticle catalysts synthesized using bioleached laterite iron as a precursor and *Citrus maxima* fruit extract and its application in the Fenton's degradation of methylene blue and rhodamine B dyes.

2. MATERIALS AND METHODS

2.1. Fruit pulp extract-based synthesis of bioleached laterite nano iron catalyst

Green synthesis of bioleached laterite nano iron catalyst (BLaNFeCs) was carried out as described in Bhaskar *et al.* 2020 (Bhaskar *et al.* 2020). Pulp of *C. maxima* was collected, washed in distilled water, and crushed to extract the juice. The juice extracted was filtered with Whatman's filter paper (No. 42) and stored at 4 °C for further use. Phytochemical extracts of *C. maxima* were added to bioleached laterite iron solution dropwise on heating at 80 °C until the color turned black. Solutions were filtered using Whatman's filter paper No. 1 and oven-dried. The extracted particles were stored in moisture-free containers. Synthesized nanoparticles were characterized using scanning electron microscopy, X-ray diffraction, electron dispersive spectrophotometry, and BET analyzer.

2.2. BLaNFeCs-based Fenton's oxidation of selective dyes

BLaNFeCs-based Fenton's degradation was carried out with an initial dye concentration of 10 mg/L for both methylene blue and rhodamine B (Dutta & Mukhopadhyay 2001). BLaNFeCs was added at an incremental dose to the dye solution taken separately in a conical flask. The solution was adjusted to a pH of 3 using 1 N H_2SO_4 and allowed to settle for 10 min to ensure proper mixing and uniform distribution of BLaNFeCs in the solution before the addition of H_2O_2. The experiment was conducted under a set of conditions for dye degradation with different dosages of BLFeNCs (0.1–1 g/L) and H_2O_2 (100–1,000 mg/L). Samples were drawn at regular intervals for analysis. During sampling, each time 1 ml of n-butanol was added to arrest the reaction (Khan *et al.* 2009). The concentration of methylene blue was measured using a UV–vis spectrophotometer. Chemical oxygen demand (COD) was measured using the calorimetric method (APHA Method 4500-F: 1992). pH was measured using a digital pH meter. Ferric iron was measured by the potassium thiocyanate method using a UV–vis spectrophotometer (Mellon & Woods 1941). H_2O_2 was measured using a UV spectrophotometer (Eisenberg 1943).

3. RESULTS AND DISCUSSION

3.1. BLaNFeCs formation and its characterization

Iron nanoparticles were formed during the reaction of fruit extract and leached laterite solution and were confirmed with SEM, XRD, and EDS analysis (Devatha *et al.* 2016; Sangami & Manu 2017). The iron particles formed were seen as spherical particles on SEM images and their size was observed to be 100–200 nm. EDS data show us three peaks corresponding to iron (Figure 1(b)) and reveal that the nanoparticles formed contain iron at 12.28% by weight composition as shown in Table 1.

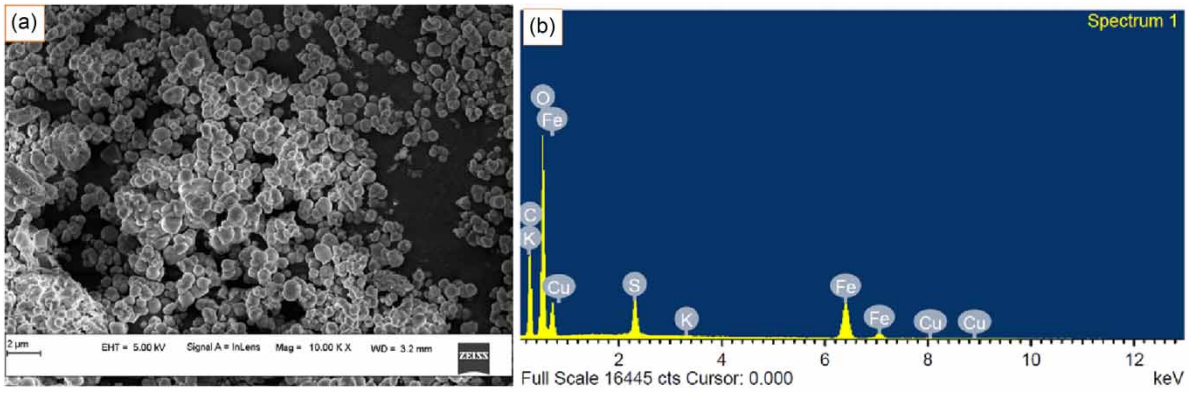

Figure 1 | Scanning electron microscopic and EDS images of BLaNFeCs showing the morphological appearance and elemental composition of synthesized nanoparticles.

Table 1 | Chemical composition of BLaFeNCs

Element	C	O	S	Fe	Cu	K
Weight %	7.10	18.92	2.02	12.28	0.08	0.08

Six peaks observed at 2θ 30.48, 35.89, 43.52, 53.99, 57.49, and 63.10 correspond to iron oxide (PDF: 01-075-0449) and 90.56 corresponds to magnesium iron gallium oxide (PDF: 00-033-0896). Broad peaks observed are due to organic material coatings stabilizing the nanoparticles and the formed nanoparticles are amorphous in nature. The low signal-to-background ratio observed shows poor crystallinity confirming the amorphous nature of nanoparticles (Chen *et al.* 2017). Chemical composition by percentage weight for formed nanoparticles is tabulated in Table 1.

BET surface areas for BLFeNPs were found to be 87.75 m^2/g with pore diameters of 7.225 nm confirming the mesoporous structure of the nanoparticles obtained (Soon & Hameed 2011) (Figure 2).

3.2. Fenton's degradation of selective dyes by BLaNFeCs

The catalytic performance of synthesized nanoparticles was confirmed by Fenton's oxidation with dye degradation efficiency of 93.6 and 91.3% for methylene blue and rhodamine B, respectively, on addition of BLaNFeCs dosage of 0.5 g/L and H_2O_2 dosage of 500 and 1,000 mg/L, respectively (Figure 3). Maximum degradation of 88.2 and 84% was observed at 40 min of treatment with a rate constant of 0.0236 and 0.020 min^{-1} for methylene blue and rhodamine B, respectively. It is observed that for methylene blue the degradation was increased by 5% with an increase in catalyst loading from 0.1 to 0.5 g/L (Figure 2). However, further increase in catalyst dosage to 1 g/L has led to a degradation drop by 8.2%. For rhodamine B, the degradation is shown to be increased by 1.3% with an increase in catalyst loading from 0.1 to 0.5 g/L and there is a decrease in efficiency by 5.3% on a further increase of catalyst loading. In all cases, treatment time is reduced by 40 min leading to maximum degradation. An increase in H_2O_2 dosage is observed to have increased the degradation efficiency up to 500 mg/L and further increase to 1,000 mg/L led to a drop in the degradation efficiency by 8.8%, indicating the scavenging effect (Khan Wirojanagud & Sermsai 2009), whereas maximum degradation of rhodamine B was observed at 1,000 mg/L of H_2O_2 dosage. It is to be noted that both for 0.5 and 1 g/L of catalyst load, the treatment time is reduced to half. An increase in catalyst load is more beneficial than increasing hydrogen peroxide since iron increases the speed of the reaction (Andrades *et al.* 2021). The result obtained is consistent

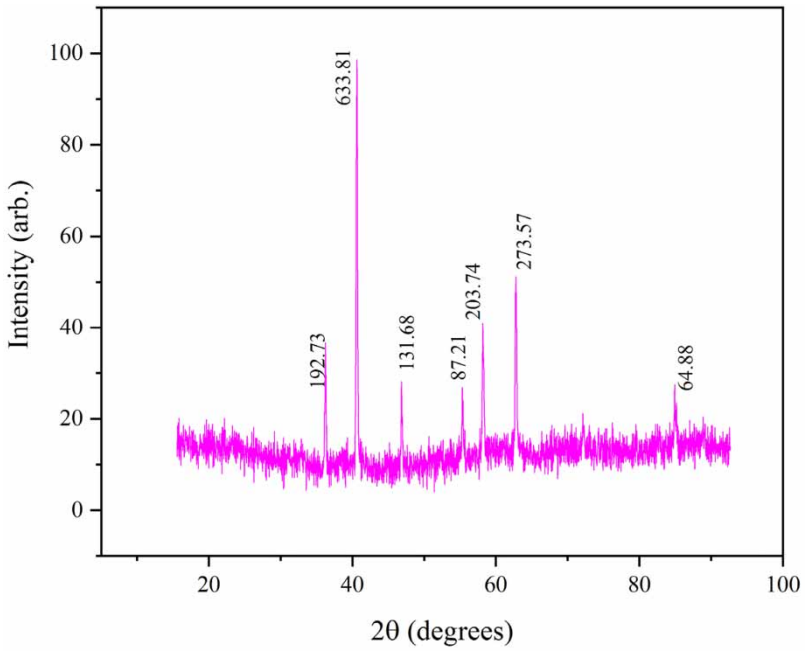

Figure 2 | XRD images of BLaNFeCs representing the corresponding peaks of synthesized nanoparticles.

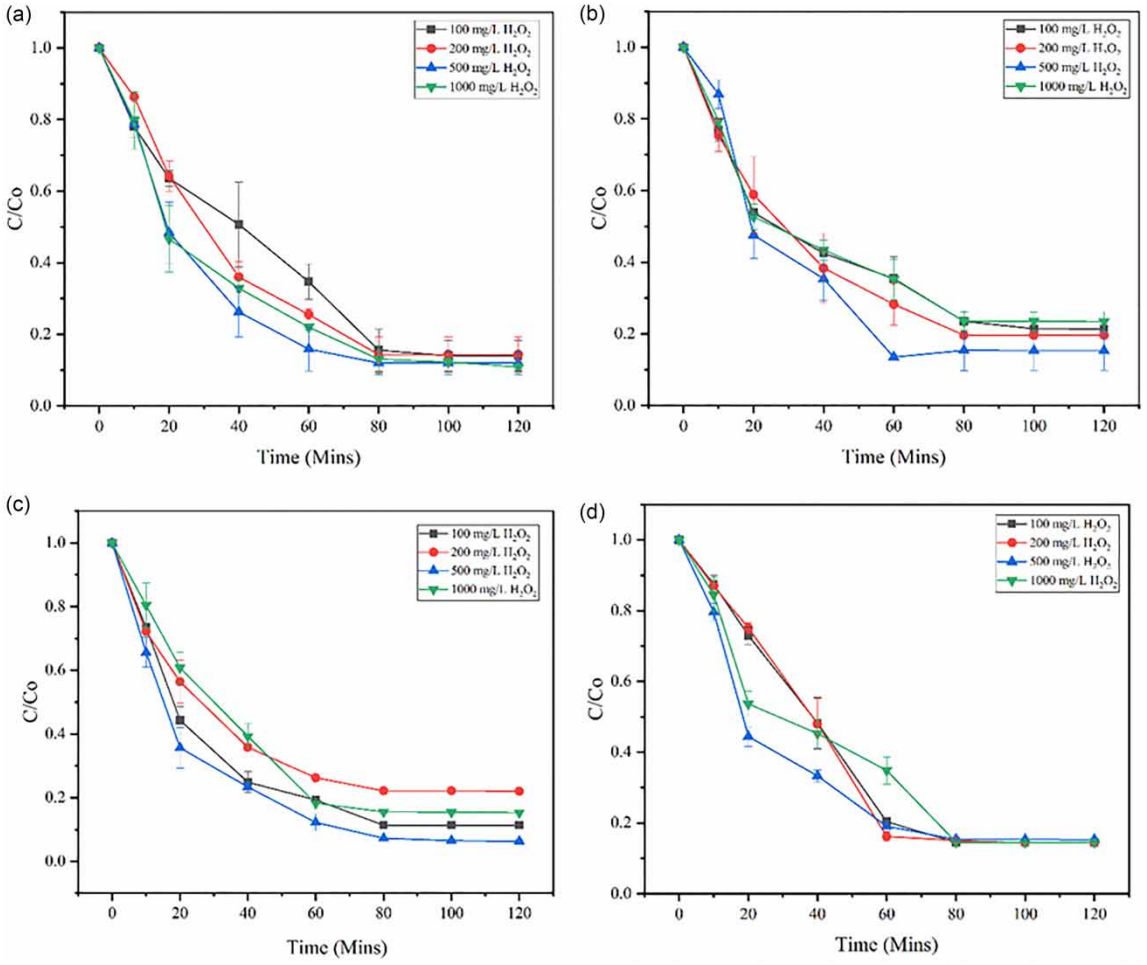

Figure 3 | Oxidative degradation of methylene blue with the following BLaNFeCs dosages: (a) 0.1 g/L; (b) 0.2 g/L; (c) 0.5 g/L; and (d) 1.0 g/L.

with previous works on the degradation of methylene blue and rhodamine B (Dutta & Mukhopadhyay 2001; Zhao & Zhu 2006; Hou *et al.* 2011; Tak *et al.* 2015; Zhou *et al.* 2016; Bishnoi *et al.* 2018; Karim *et al.* 2022).

The degradation mechanism of methylene blue and rhodamine B was demonstrated by previous researchers. Degradation of methylene blue involves the breaking of the C–N bond connected to the benzene ring generating degradation products, namely H_2SO_4 and HCl (Amini *et al.* 2015). Degradation of Rhodamine B follows N-de-ethylation, chromophore cleavage, ring opening, and mineralization stages. Zhou & co-workers (2016) identified three intermediate products due to the de-ethylating steps of N,N′-diethylammonium groups as N,N, N′-triethyl rhodamine, N,N′-diethyl rhodamine, and rhodamine (Zhou *et al.* 2016). Hou *et al.* (2011) claim oxalic acid, formic acid, and acetic acid as chromophore cleavage and ring opening intermediates. Tertiary amines formed during the degradation can be oxidized to amine oxides which further oxidize to aldehyde intermediates and then to carboxylic acids (Hou *et al.* 2011) (Figure 4).

Variation of iron and decolorization of methylene blue and rhodamine B during Fenton's oxidation are presented in Figures 5 and 6. It is observed from the graph that the ferrous form of iron leached out of nanocatalyst undergoes an oxidation process forming the ferric iron species which is confirmed with iron determination (Figures 5(a) and 6(a)) and later there is a drop in the ferric form of iron in the solution. Observed results are consistent with previous works (Khan *et al.* 2009; Bhaskar *et al.* 2019, 2021; Bhaskar, Basavaraju Manu 2020). Figures 5(b) and 6(b) present the decolorization efficiency during the oxidation process which is indicated by COD reduction (Dutta & Mukhopadhyay 2001). The maximum reduction in COD observed was 87.6 and 81.5% for the optimum degradation of methylene blue and rhodamine B, respectively. The reduction in COD is also attributed to the adsorption process other than Fenton's oxidation (Masomboon 2009). Complete degradation was observed within 40 min of treatment. Fenton's treatment is shown to be active in acidic pH.

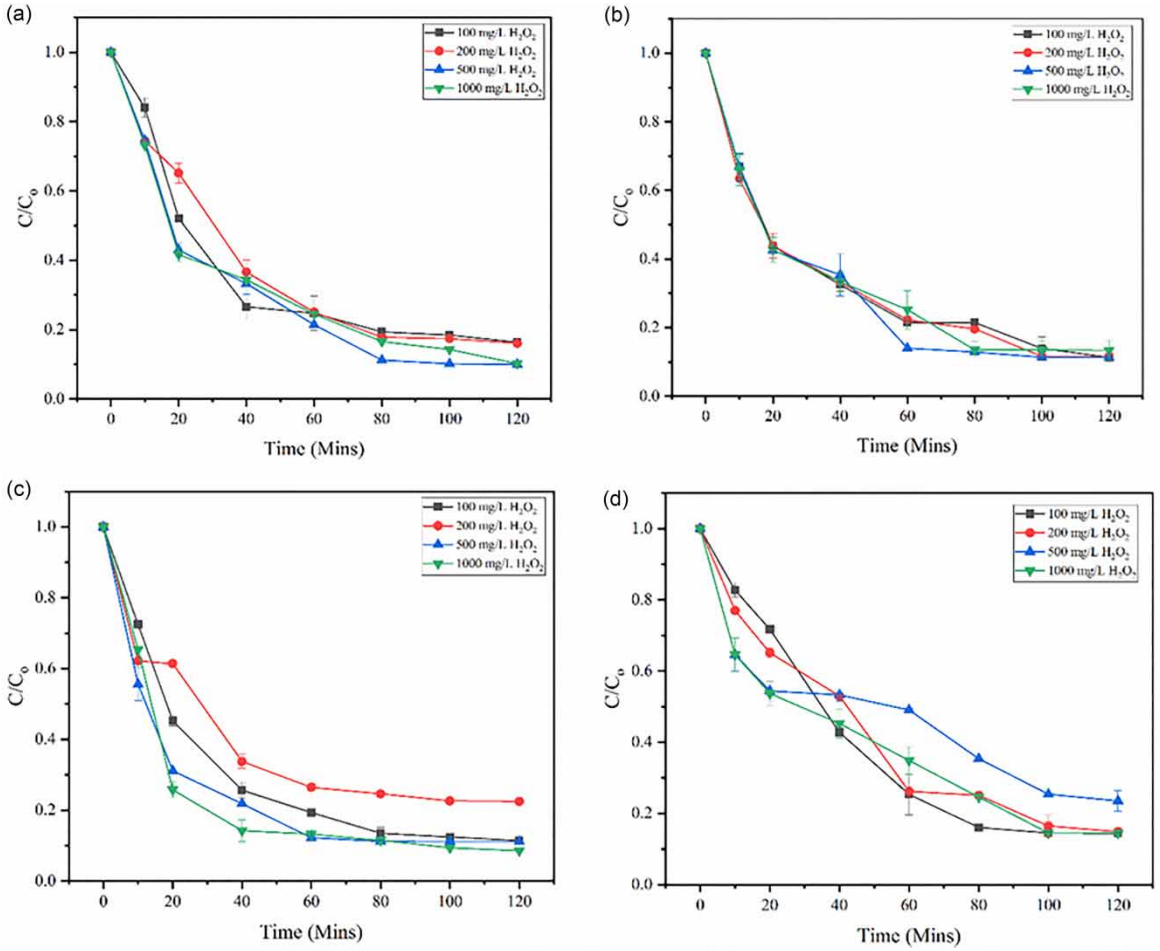

Figure 4 | Oxidative degradation of rhodamine B with the following BLaNFeCs dosages: (a) 0.1 g/L; (b) 0.2 g/L; (c) 0.5 g/L; and (d) 1.0 g/L.

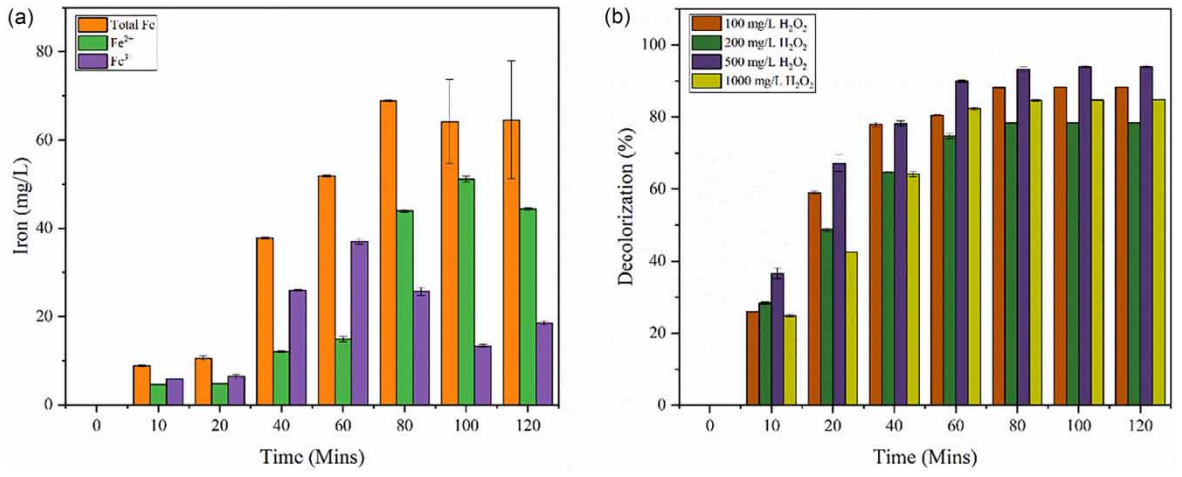

Figure 5 | (a) Variation of iron and (b) decolorization efficiency of methylene blue during Fenton's oxidation.

During the Fenton's process, hydrated ferrous ions get transformed into the colloidal ferric species forming the ferric hydroxyl complexes, thereby reducing the efficiency at basic pH. During the study, pH varied slightly from 3.0 to 4.4 which favored the oxidation process forming hydroxyl radicals (Kang & Hwang 2000; Burbano *et al.* 2005). It is to be noted that the rate of oxidation in Fenton's process depends on the dissolution rate of ferrous iron that has leached out of the nanocatalyst. The amount of catalyst increases the degradation efficiency which

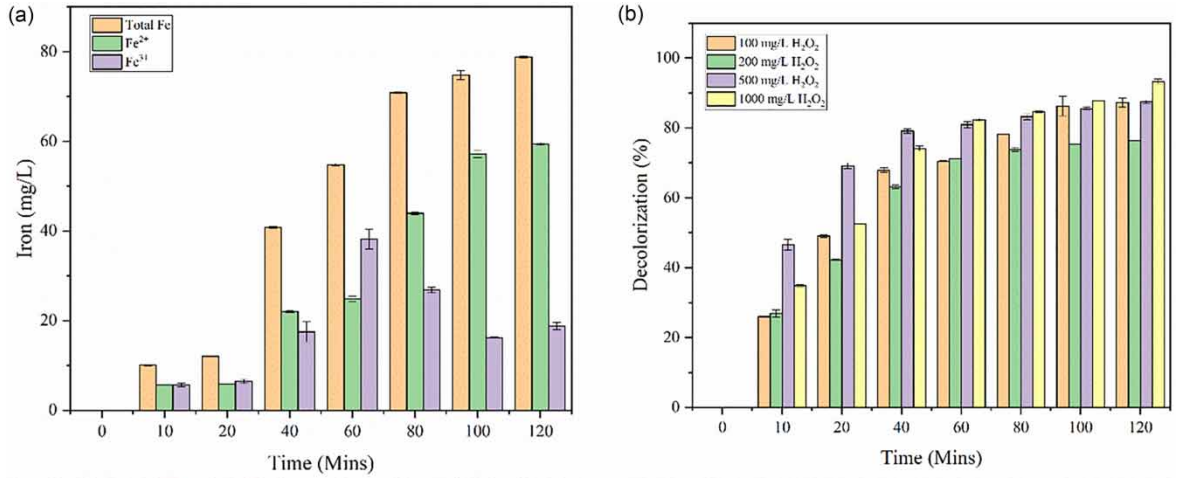

Figure 6 | (a) Variation of iron and (b) decolorization efficiency of rhodamine B during Fenton's oxidation.

might be due to adsorption on the surface of the nanocatalyst particles, making the process heterogenous in reaction (Barbusiński 2005). Figure 7 indicates the linear fit for the Fenton's oxidation of methylene blue and rhodamine B follows a pseudo-first-order kinetics with a rate constant of 0.0236 and 0.020 min^{-1}, respectively. The reusability of spent catalyst was studied for the Fenton's oxidation of methylene blue. Degradation of methylene blue is amenable to spent catalyst reuse. Figure 8 shows us the degradation of methylene blue in catalyst reuse. Degradation on the first cycle of reuse was 92.0% with a rate constant of 0.0188 min^{-1}, whereas on the second cycle of reuse the efficiency was 88.4% with a rate constant of 0.0159 min^{-1}. For the third cycle of reuse, degradation efficiency was 73.4% with a rate constant of 0.0102 min^{-1}. For the fourth and fifth cycles of reuse, degradation efficiencies were 64.5 and 68.8% with rate constants of 0.0088 and 0.0086 min^{-1}, respectively. It is observed that the degradation efficiency is decreasing on catalyst reusage with a decrease in the rate constant. The drop in degradation might be due to the loss of iron from nanoparticles by leaching in each cycle. However, it is observed that the catalyst can be reused for three consecutive cycles (Table 2).

4. CONCLUSIONS

Iron nanocatalyst was sustainably synthesized by a phytochemical method using bioleached laterite iron as a percussor and *C. maxima* fruit extract. Fenton's oxidation of methylene blue and rhodamine B dyes has been carried out using a synthesized nano iron catalyst for the evaluation of its potential as a Fenton's catalyst in the degradation of dyes. It is observed that at acidic pH synthesized nanocatalyst is proven for its catalytic role in dye degradation with degradation efficiency of 93.6 and 91.3% with 1:1 and 1:2 BLaNFeCs:H_2O_2 ratio for methylene blue and rhodamine B, respectively. Degradation lasts for 80 min with a maximum degradation in 40 min

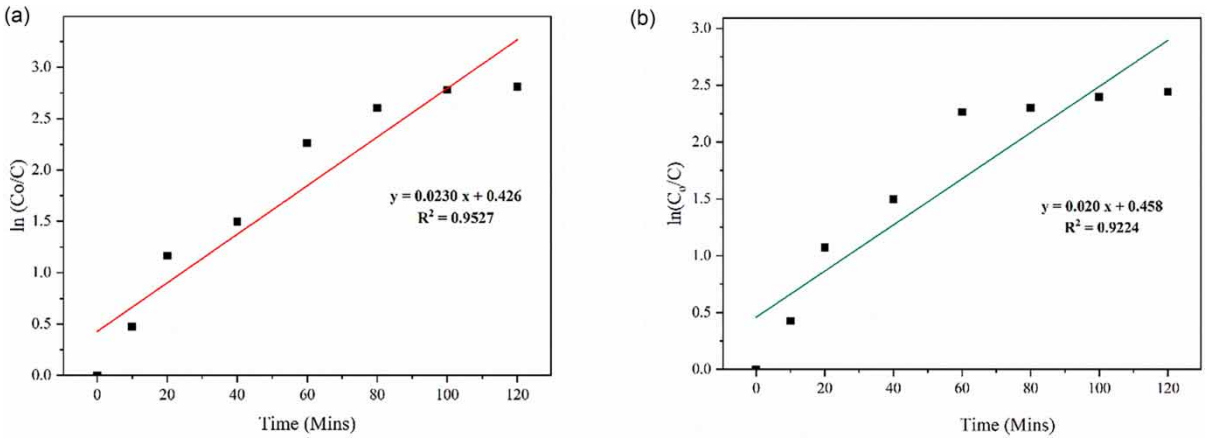

Figure 7 | Linear fit for Fenton's oxidation of (a) methylene blue and (b) rhodamine B using BLaNFeCs.

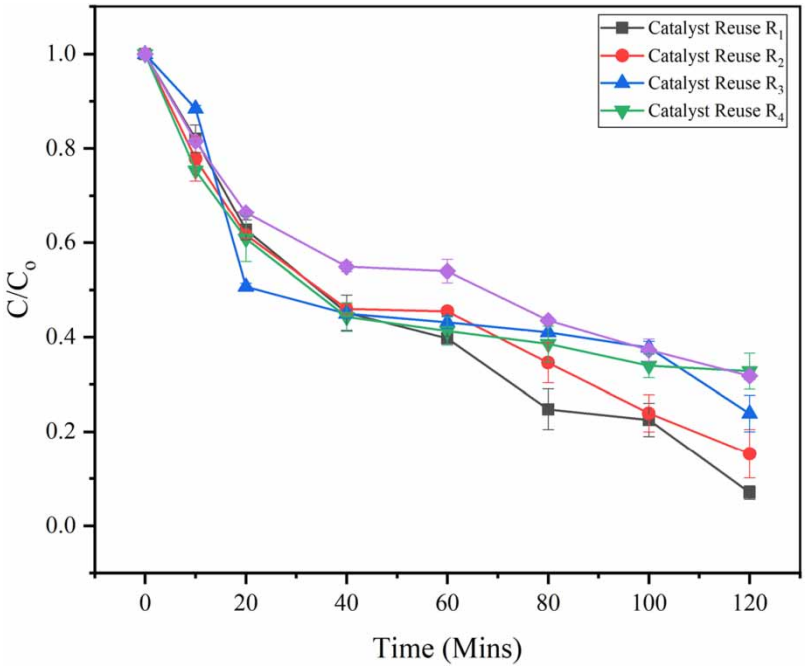

Figure 8 | Catalyst reusability on Fenton's oxidation of methylene blue using BLaNFeCs.

Table 2 | Overview of Fenton's oxidation of selective dyes in water

	Operating parameter					
Target compound	**BLaFeNCs (g/L)**	**H_2O_2 Dosage (mg/L)**	**Degradation (%)**	**COD removal (%)**	**Rate constant *k* (min^{-1})**	**Regression R^2**
Methylene blue	0.5	500	93.6	87.6	0.0236	0.9177
Rhodamine B	0.5	1000	91.3	81.5	0.0200	0.9224

following a pseudo-first-order kinetics with rate constants of 0.0236 and 0.020 min^{-1}. An increase in catalyst dose led to a shortening of treatment time with an increase in degradation efficiency. Reusability tests confirm that spent catalyst can be reused for three consecutive cycles with better efficiency in dye removal. The study confirms the sustainable use of natural laterite iron-based nanoparticles as a catalyst in Fenton's degradation of dyes.

DATA AVAILABILITY STATEMENT

All relevant data are included in the paper or its Supplementary Information.

CONFLICT OF INTEREST

The authors declare there is no conflict.

REFERENCES

Amini, M., Ashrafi, M., Gautam, S. & Chae, K. H. 2015 Rapid oxidative degradation of methylene blue by various metal oxides doped with vanadium. *RSC Advances* **47**, 37469–37475.

Andrades, J. A., Coello, M. D., Quiroga, J. M. & Lojo-l, M. 2021 Degradation of simazine by photolysis of hydrogen peroxide fenton and photo-Fenton under darkness, sunlight and UV light. *Journal of Water Process Engineering* **42** (March), 102–115.

APHA 1992 *Standard Methods for the Examination of Water and Wastewater*, 18th edn. APHA, Washington, DC, p. 552.

Barbusiński, K. 2005 The modified Fenton process for decolorization of dye wastewater. *Polish Journal of Environmental Studies* **14** (3), 281–285.

Bhaskar, S., Manu, B. & Sreenivasa, M. Y. 2019 Bacteriological synthesis of iron hydroxysulfate using an isolated acidithiobacillus ferrooxidans strain and its application in Ametryn degradation by Fenton's oxidation process. *Journal of Environmental Management* **232**, 236–242.

Bhaskar, S., Manu, B. & Sreenivasa, M. Y. 2020 Bioleaching of Iron from fly ash using a novel isolated Acidithiobacillus ferrooxidans strain and evaluation of catalytic role of leached iron in the Fenton's oxidation of cephelaxin. *Journal of the Indian Chemical Society* **97** (3), 360–367.

Bhaskar, S., Manu, B. & Sreenivasa, M. Y. 2021 Green synthesis of bioleached flyash iron nanoparticles (GBFFeNP) using azadirachta indica leaves and its application as fenton's catalyst in the degradation of dicamba. In *Recent Trends in Civil Engineering* (A. Sil, D-P. N. Kontoni & R. K. Pancharathi, eds.) Springer, Singapore, pp. 365–371.

Bishnoi, S., Kumar, A. & Selvaraj, R. 2018 Facile synthesis of magnetic iron oxide nanoparticles using inedible cynometra rami Fl Ora fruit extract waste and their photocatalytic degradation of methylene blue dye. *Materials Research Bulletin* **97** (March 2017), 121–127. https://doi.org/10.1016/j.materresbull.2017.08.040.

Burbano, A. A., Dionysiou, D. D., Suidan, M. T. & Richardson, T. L. 2005 Oxidation kinetics and effect of PH on the degradation of MTBE with fenton reagent. *Water Research* **39**, 107–118.

Chen, F., Xie, S., Huang, X. & Qiu, X. 2017 Ionothermal synthesis of Fe_3O_4 magnetic nanoparticles as efficient heterogeneous fenton-like catalysts for degradation of organic pollutants with H_2O_2. *Journal of Hazardous Materials* **322**, 152–162. http://dx.doi.org/10.1016/j.jhazmat.2016.02.073.

Devatha, C. P., Thalla, A. K. & Katte, S. Y. 2016 Green synthesis of iron nanoparticles using different leaf extracts for treatment of domestic waste water. *Journal of Cleaner Production* **139**, 1425–1435. http://dx.doi.org/10.1016/j.jclepro.2016.09.019.

Dutta, K. & Mukhopadhyay, S. 2001 Chemical oxidation of methylene blue using a fenton-like reaction. *Journal of Hazardous Materials* **84**, 57–71.

Eisenberg, G. M. 1943 Colorimetric determination of hydrogen peroxide. *Industrial and Engineering Chemistry* **5**, 327–328.

Hou, M. F., Liao, L., Zhang, W. D., Tang, X. Y., Wan, H. F. & Yin, G. C. 2011 Degradation of Rhodamine B by Fe (0) -Based fenton process with H_2O_2. *Chemosphere* **83** (9), 1279–1283. http://dx.doi.org/10.1016/j.chemosphere.2011.03.005.

Huang, C. P., Dong, C. & Tang, Z. 1993 Advanced chemical oxidation: its present role and potential future in hazardous waste treatment. *Waste Management* **13**, 361–377.

Huang, Y.-h., Huang, Y.-f., Chang, P.-s. & Chen, C.-y. 2008 Comparative study of oxidation of dye-reactive black B by different advanced oxidation processes : Fenton, electro-fenton and photo-fenton. *Journal of hazardous materials* **154**, 655–662.

Islam, M. R. & Mostafa, M. G. 2018 Textile dyeing effluents and environment concerns – a review. *Journal of Environmental Science and Natural Resources* **11**, 131–144.

Kang, Y. U. N. W. & Hwang, K.-y. 2000 Effects of reaction conditions on the oxidation efficiency in the Fenton process. *Water Research* **34** (10), 2786–2790.

Karim, A. V., Hassani, A., Eghbali, P. & Nidheesh, P. V. 2022 Nanostructured modified layered double hydroxides (LDHs) -based catalysts : a review on synthesis, characterization, and applications in water remediation by advanced oxidation processes. *Current Opinion in Solid State & Materials Science* **26** (1), 100965. https://doi.org/10.1016/j.cossms.2021.100965.

Khan, E., Wirojanagud, W. & Sermsai, N. 2009 Effects of iron type in Fenton reaction on mineralization and biodegradability enhancement of hazardous organic compounds. *Journal of Hazardous Materials* **161**, 1024–1034.

Kim, J. R. & Kan, E. 2014 Journal of industrial and engineering chemistry heterogeneous photo-Fenton oxidation of methylene blue using cds-Carbon nanotube/TiO_2 under visible light. *Journal of Industrial and Engineering Chemistry*. Http://dx.doi.org/10.1016/j.jiec.2014.03.032.

Kim, T.-h., Park, C., Yang, J. & Kim, S. 2004 Comparison of disperse and reactive dye removals by chemical coagulation and Fenton oxidation. *Journal of hazardous materials* **112**, 95–103.

Masomboon, N. 2009 Chemical oxidation of 2, 6-dimethylaniline in the fenton process. *Environmental Science & Technology* **43** (22), 8629–8634.

Mellon, J. T. & Woods, M. G. 1941 Thiocyanate Method for Iron. *Industrial & Engineering Chemistry Analytical Edition* **13** (8), 551–554.

Nour, A. n.d. *Efficacy of Methylene Blue Dye in Localization of Sentinel*.

Sangami, S. & Manu, B. 2017 Synthesis of green iron nanoparticles using laterite and their application as a fenton. *Environmental Technology & Innovation*. http://dx.doi.org/10.1016/j.eti.2017.06.003.

Simmons, R., Thevarajah, S., Brennan, M. B., Christos, P. & Osborne, M. 2003 Methylene blue dye as an alternative to isosulfan blue dye for sentinel lymph node localization. *Annals of Surgical Oncology* **10** (3), 242–247.

Soon, A. N. & Hameed, B. H. 2011 Heterogeneous catalytic treatment of synthetic dyes in aqueous media using Fenton and photo-assisted Fenton process. *Desalination* **269** (1–3), 1–16. http://dx.doi.org/10.1016/j.desal.2010.11.002.

Tak, B. Y., Tak, B. S., Kim, Y. J., Park, Y. J., Yoon, Y. H. & Min, G. H. 2015 Optimization of color and COD removal from livestock wastewater by electrocoagulation process : application of Box – Behnken Design (BBD). *Journal of Industrial and Engineering Chemistry* **28**, 307–315.

Zhao, X. U. & Zhu, Y. 2006 Synergetic degradation of Rhodamine B at a porous $ZnWO_4$ film electrode by combined electro-oxidation and photocatalysis. *Environmental Science & Technology* **40** (10), 3367–3372.

Zhou, W., Zhao, H., Gao, J., Meng, X., Wu, S. & Qin, Y. 2016 Influence of a reagents addition strategy on the Fenton oxidation of Rhodamine B : control of the competitive reaction of .OH †. *RSC Advances* **6** (3), 108791–108800.

First received 2 September 2022; accepted in revised form 28 October 2022. Available online 9 November 2022